High-Order Maps for Realistic RF Cavities and Accelerator Simulation

Dan T. Abell, Ilya V. Pogorelov, Peter H. Stoltz

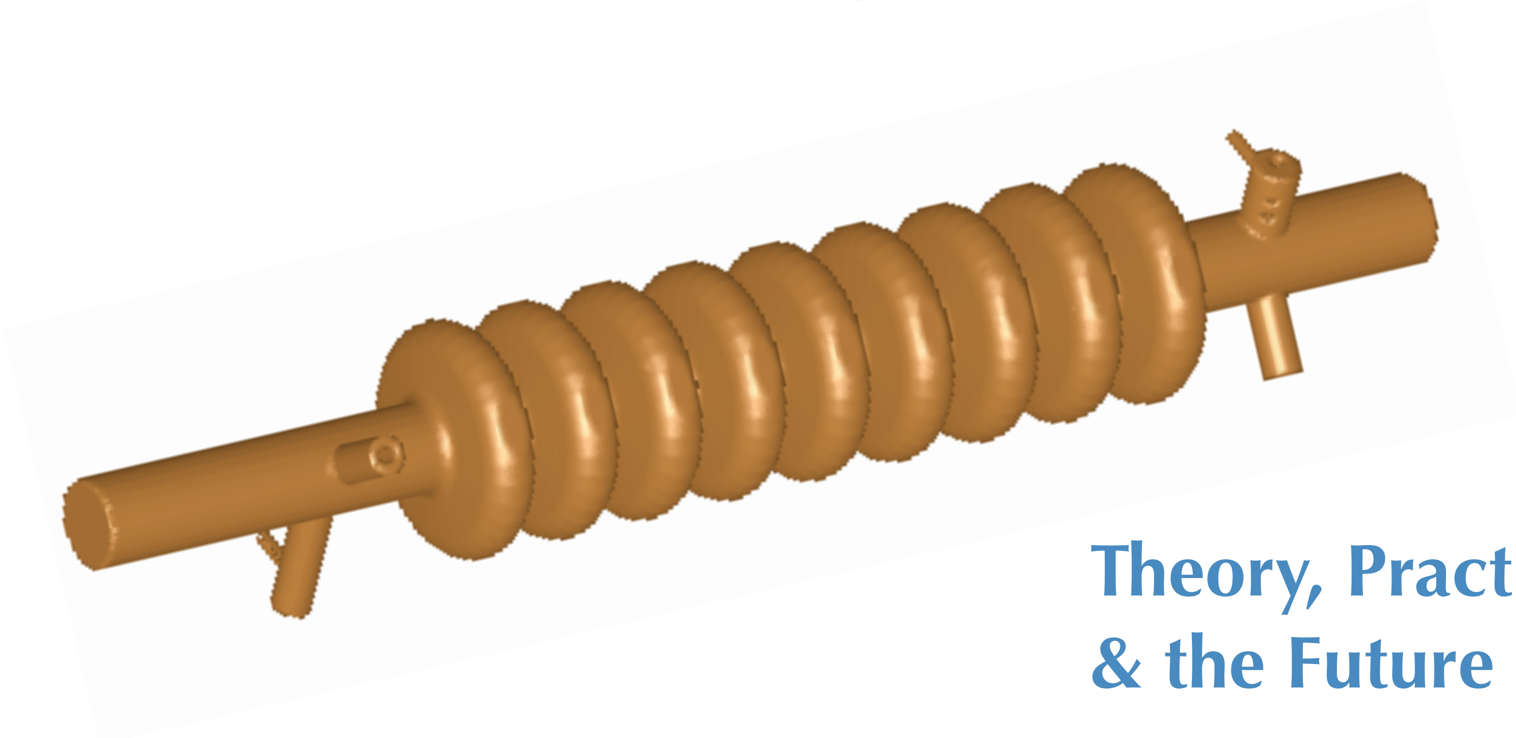

Theory, Practise, & the Future

This work was supported in part by the US Department of Energy, Office of Science, Office of Nuclear Physics, under SBIR Grant No. DE-FG02-06ER84485.

Transfer maps for realistic elements require high-order derivatives of on-axis fields

Mid 1980s: Dragt, Forest, and Ryne developed the MARYLIE GENMAP routines. Mid 1990s: Venturini and Dragt showed how to compute accurate transfer maps for realistic magnets.

A.J. Dragt and E. Forest, *J. Math. Phys.* **24** 2734, 1983. R.D. Ryne and A.J. Dragt, *PAC 1987, 1081*. M. Venturini and A.J. Dragt, *Nucl. Instrum. Methods Phys. Res., Sect. A* **427** 387–392, 1999.

$$H = -\sqrt{p_t^2/c^2 - (\mathbf{p}_\perp - q\mathbf{A}_\perp)^2} - qA_z$$

require accurate vector potential to insert into the Hamiltonian; coefficients are *generalized gradients*

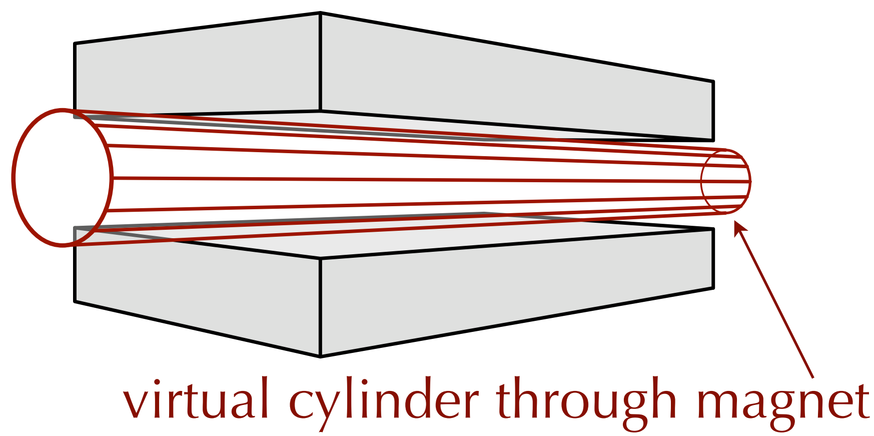

Fit surface data to compute interior data: reduced sensitivity to noise/errors.

C.E. Mitchell and A.J. Dragt, *ICAP 2006, Chamonix, France*, 198–200.

Other geometries include bent box (Dragt and Walstrom, *PAC 2001*).

Finite Structure: Use Fourier transform rep. for electric field E (vec. Helmholtz eqn.)

General representation is given in terms of hybrid Bessel functions, $R_m(k,r)$ and characteristic functions.

$$
\begin{aligned}
E_\rho(\mathbf{r}) = \int_{-\infty}^{\infty} \frac{dk}{\sqrt{2\pi}} e^{ikz} \left(-\frac{ik}{\kappa_l}\right) \Bigg\{ \tilde{e}_0(k) R_1(k,\rho) + \sum_{m=1}^{\infty} \Bigg[\left(\tilde{e}_m(k) R_{m+1}(k,\rho) + \tilde{\beta}_m(k) \frac{R_m(k,\rho)}{\kappa_l \rho} \right) \cos(m\phi) \\
+ \left(\tilde{f}_m(k) R_{m+1}(k,\rho) + \tilde{\alpha}_m(k) \frac{R_m(k,\rho)}{\kappa_l \rho} \right) \sin(m\phi) \Bigg] \Bigg\},
\end{aligned}
$$

$$
\begin{aligned}
E_\phi(\mathbf{r}) = \int_{-\infty}^{\infty} \frac{dk}{\sqrt{2\pi}} e^{ikz} \left(\frac{ik}{\kappa_l}\right) \Bigg(\tilde{f}_0(k) R_1(k,\rho) + \sum_{m=1}^{\infty} \Bigg\{ \Bigg[\tilde{f}_m(k) R_{m+1}(k,\rho) + \tilde{\alpha}_m(k) \left(\frac{R_m(k,\rho)}{\kappa_l \rho} - \frac{1}{m} R_{m-1}(k,\rho) \right) \Bigg] \cos(m\phi) \\
- \Bigg[\tilde{e}_m(k) R_{m+1}(k,\rho) + \tilde{\beta}_m(k) \left(\frac{R_m(k,\rho)}{\kappa_l \rho} - \frac{1}{m} R_{m-1}(k,\rho) \right) \Bigg] \sin(m\phi) \Bigg\} \Bigg),
\end{aligned}
$$

$$
E_z(\mathbf{r}) = \int_{-\infty}^{\infty} \frac{dk}{\sqrt{2\pi}} e^{ikz} \left\{ \tilde{e}_0(k) R_0(k,\rho) + \sum_{m=1}^{\infty} \left[\tilde{e}_m(k) R_m(k,\rho) \cos(m\phi) + \tilde{f}_m(k) R_m(k,\rho) \sin(m\phi) \right] \right\}.
$$

Characteristic functions determine *this* mode in *this* cavity.
We extract them from inverse FTs of surface field data.

Coefficients in the transverse expansion of E (hence A) are *generalized gradients*

Example: For an azimuthally symmetric accelerating mode, the longitudinal field has the form

$$E_z(\mathbf{r}) = \int_{-\infty}^{\infty} \frac{dk}{\sqrt{2\pi}} e^{ikz} \tilde{e}_0(k) R_0(k,\rho) = \sum_{j=0}^{\infty} \frac{(\rho/2)^{2j}}{(j!)^2} \underbrace{\int_{-\infty}^{\infty} \frac{dk}{\sqrt{2\pi}} e^{ikz} (k^2 - k_l^2)^j \tilde{e}_0(k)}_{\left(-\frac{d^2}{dz^2} - k_l^2\right)^j E_z(\rho=0,z)} .$$

expand in powers of ϱ

generalized gradients

The vector potential differs only by a factor of $i\omega_l$.

D.T. Abell, *Phys. Rev. ST Accel. Beams* **9** 052001, 2006.

Fitting to surface data damps noise/errors: D^6, even with 10% (relative) surface noise

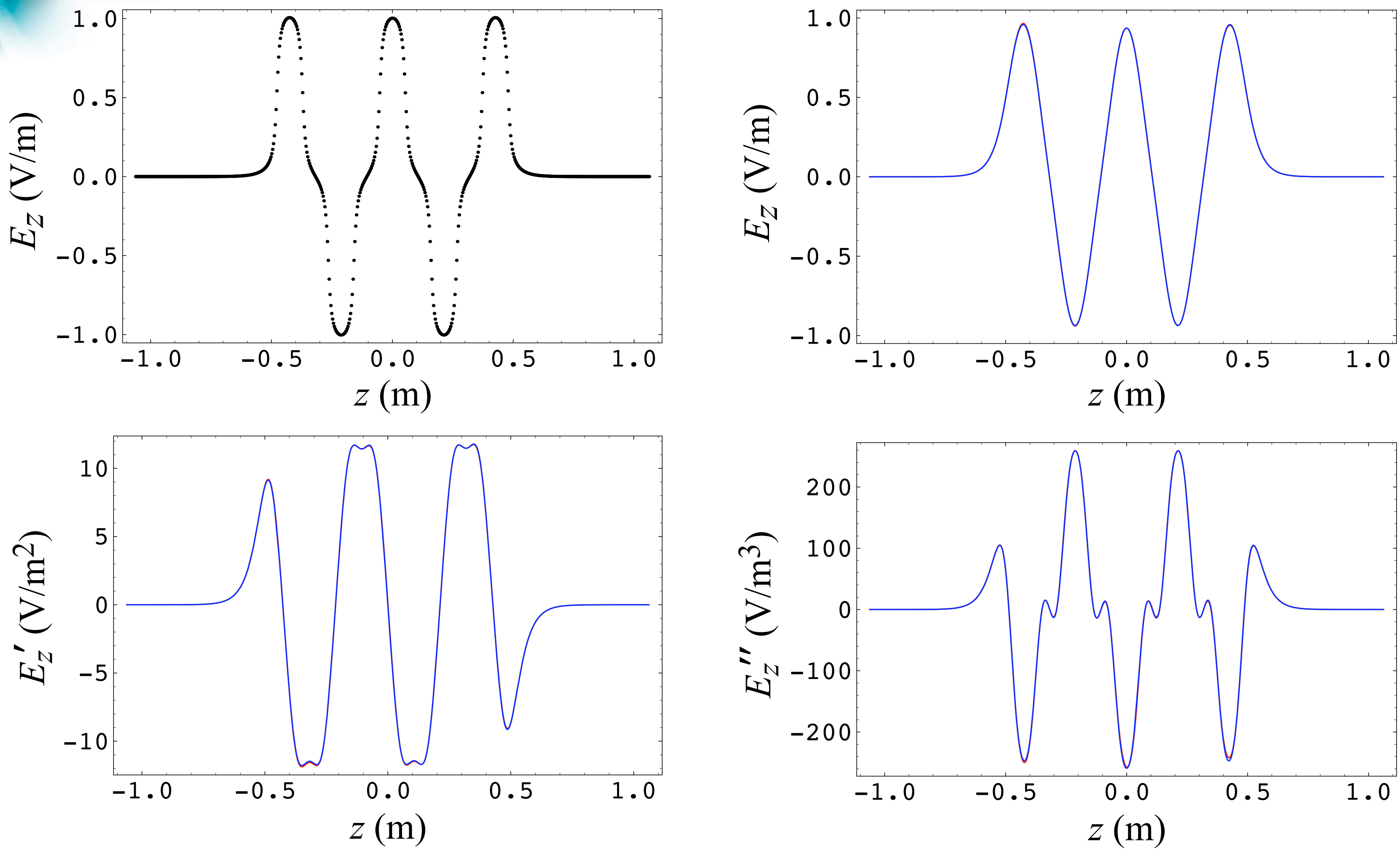

Fitting to surface data damps noise/errors (cont.)

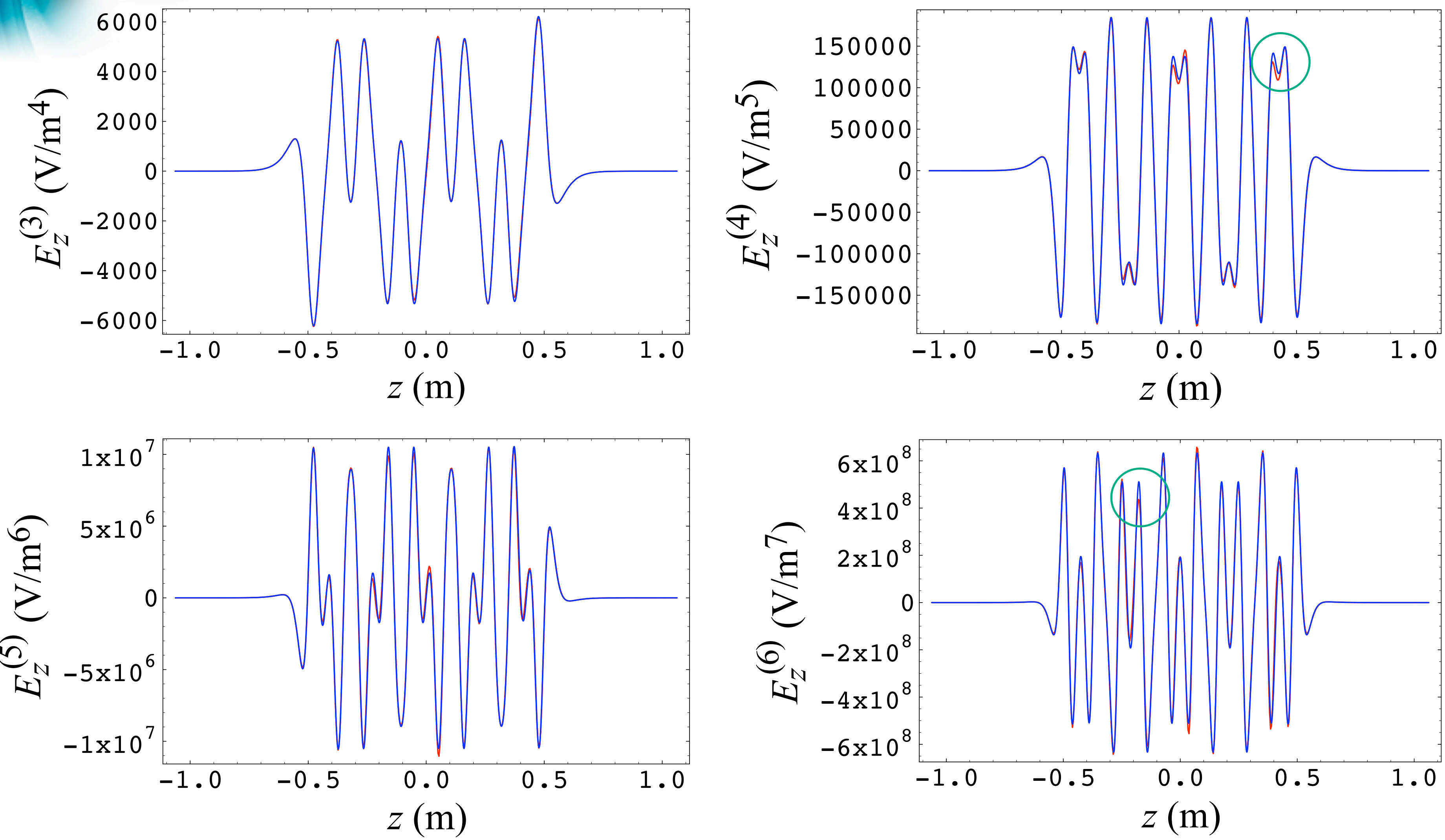

To obtain surface field data, we use VORPAL and a powerful new mode analysis technique

C. Nieter and J.R. Cary, *J. Comput. Phys.* **196** 448–493, 2004.
G.R. Werner and J.R. Cary, *J. Comput. Phys.* **227** 5200, 2008.

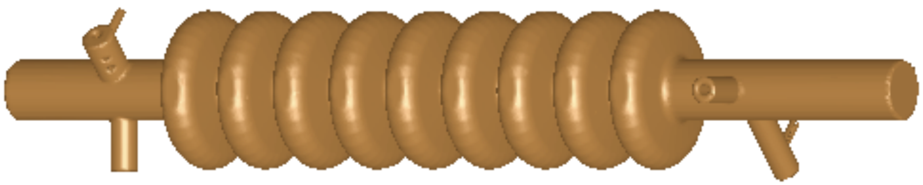

Nine-cell ILC crab cavity: includes LOM and SOM couplers, as well as flats that introduce a 10 MHz split between the dominant dipole modes.

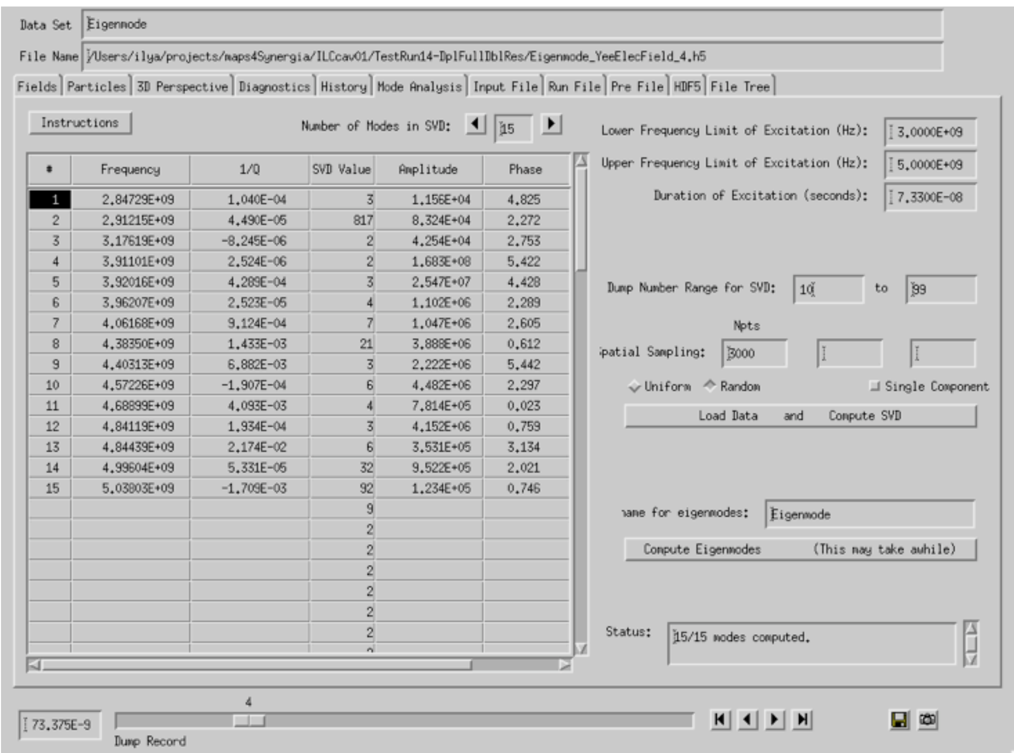

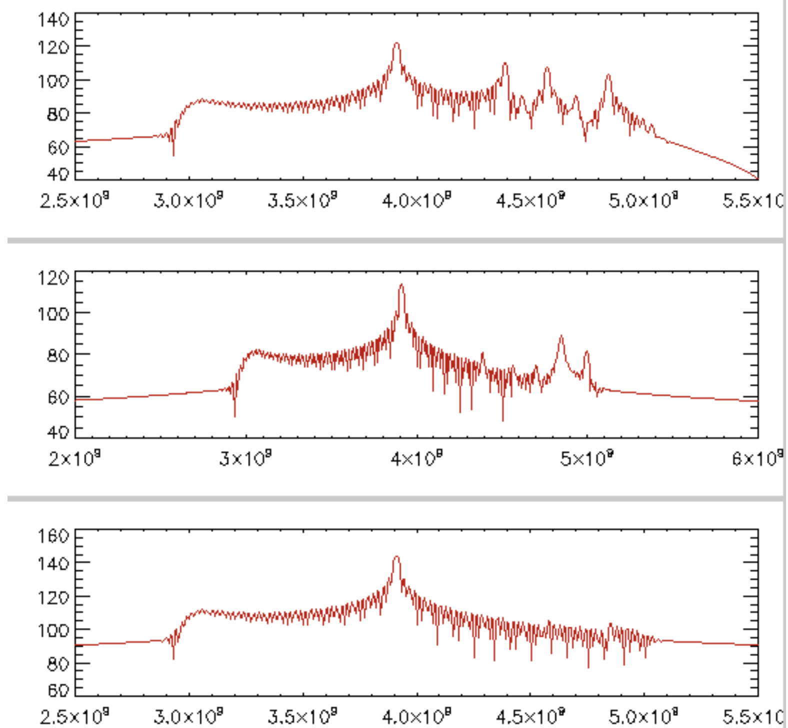

To obtain surface field data, we use VORPAL and a powerful new mode analysis technique

C. Nieter and J.R. Cary, *J. Comput. Phys.* **196** 448–493, 2004.
G.R. Werner and J.R. Cary, *J. Comput. Phys.* **227** 5200, 2008.

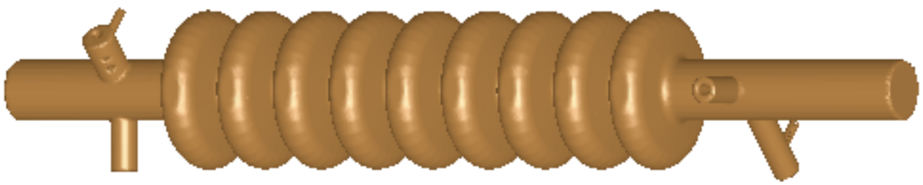

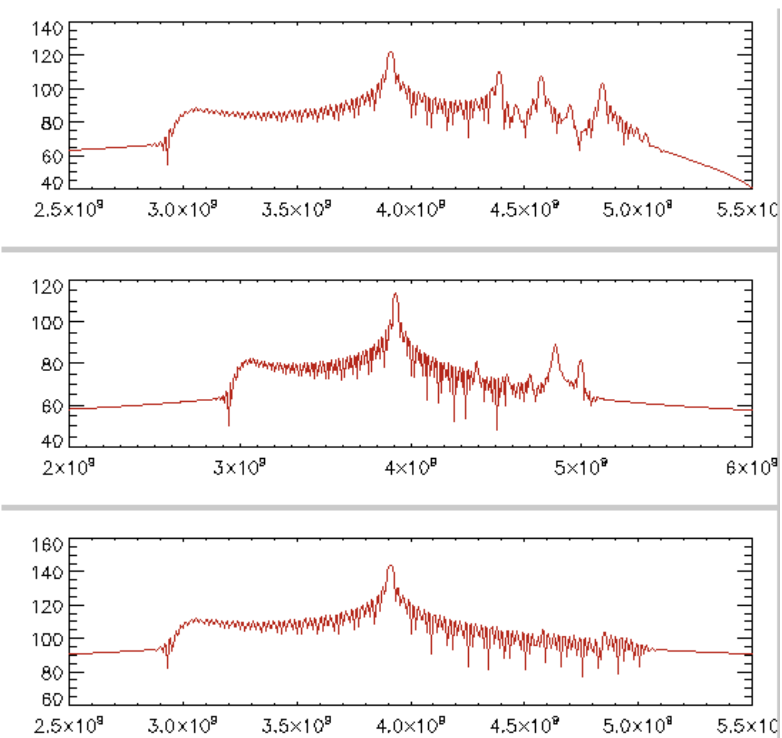

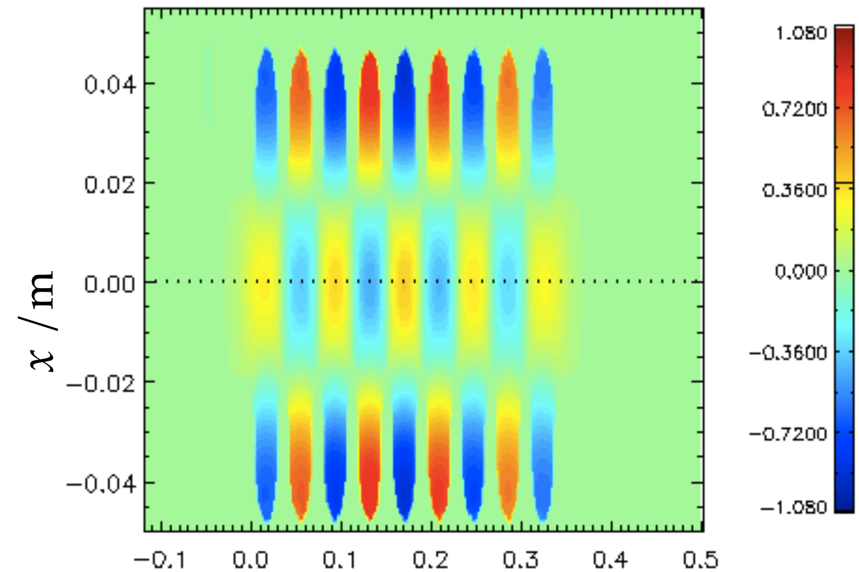

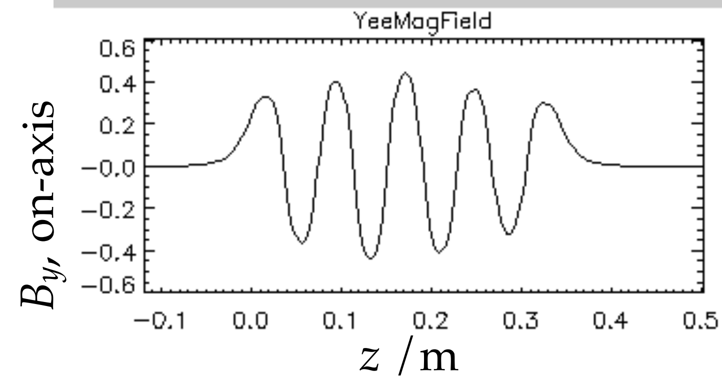

We now have results for realistic maps of particles traversing ILC crab cavities

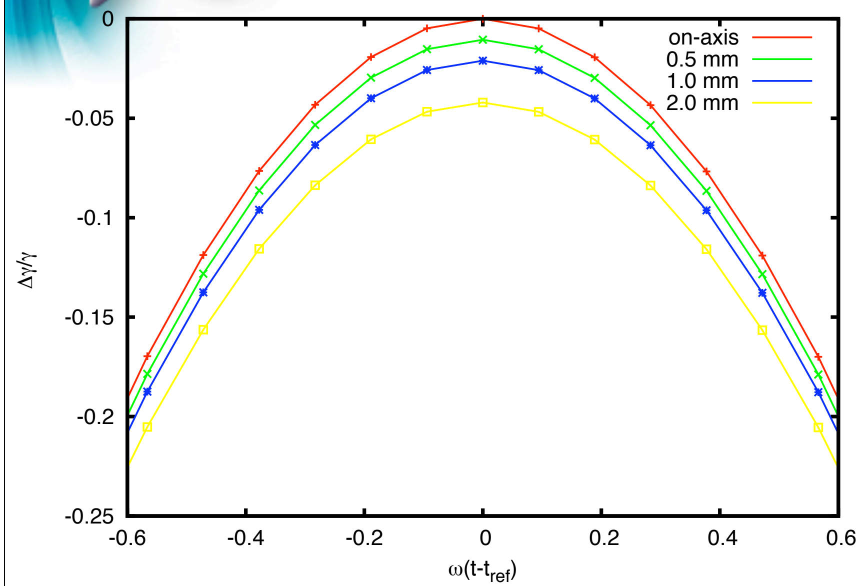

Relative energy variation for particles with different offsets. (Phase set such that reference particle receives no net kick.)

Cumulative p_x and p_y for 250GeV electron bunch. σ_z=300μm, and rotation 7mrad

Cumulative p_x for long bunch.

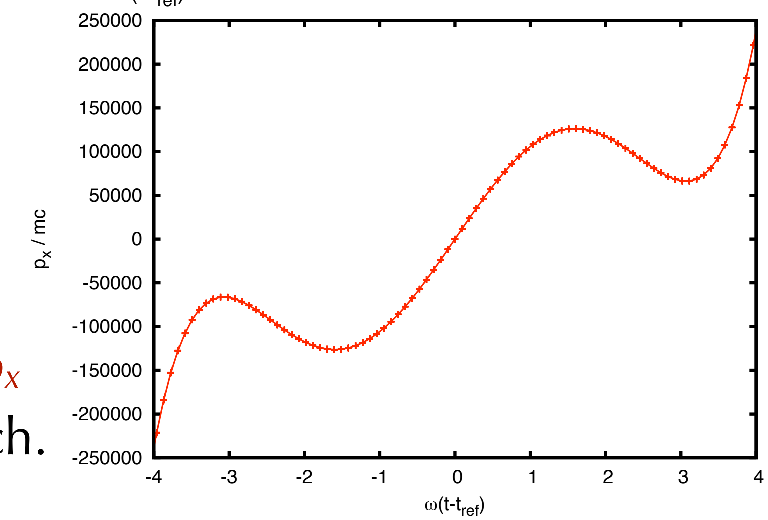

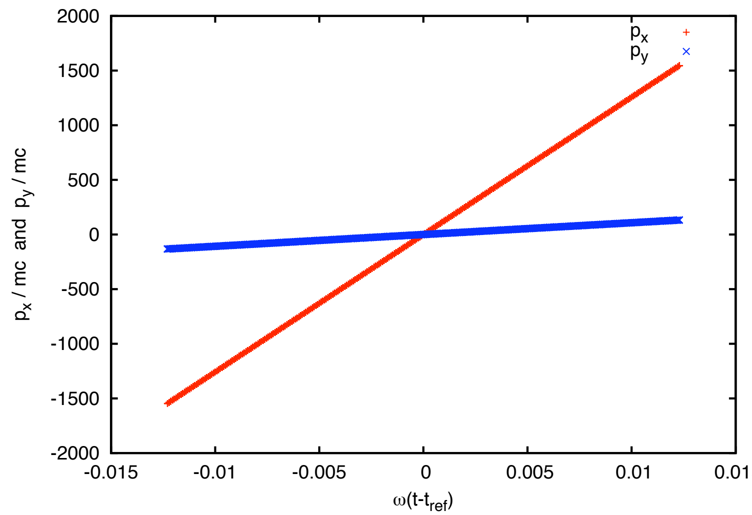

Summary

A knowledge of field values on the surface of a virtual cylinder that passes through an rf cavity makes it possible to compute accurate and high-order generalized gradients—hence accurate expansions of the fields and vector potentials—in the interior of an rf structure. This extraction of generalized gradients is robust in the presence of noise.

The ML/I type code egengrad implements this capability.

With the GENMAP capability of ML/I, we convert the generalized gradients into transfer maps. The generalized gradients we compute just once. The maps must be recomputed for different cavity phase settings.

The ML/I type code nlrf implements this capability.

Summary (cont.)

The technique described here applies not just to axi-symmetric accelerating modes, but to very general field profiles. This allows it to take into account the distortions caused by various couplers and other variations of the ideal geometry.

The new filter diagonalization method (FDM), implemented in VORPALVIEW, makes it possible to extract reliable mode profiles from an electromagnetic simulation.

The Future is Now

It is possible to superpose modes by adding the corresponding vector potentials before running GENMAP. Because the relative phases will change from turn to turn, this will require recomputing the map on each turn. For large parallel computations, do this on one node, while other nodes are pushing particles around the lattice.

This will allow one to explore, for example, how well we must suppress undesired modes.